

# RECENT PROGRESS IN MODELING BOTTOM-INTERACTING SOUND PROPAGATION WITH PARABOLIC EQUATIONS

Ding Lee  
Naval Underwater Systems Center  
New London, CT 06320

Kenneth E. Gilbert  
Naval Ocean Research & Development Activity  
NSTL Station, MS 39529

## Abstract

In 1973 Tappert introduced the parabolic equation (PE) into underwater acoustics, along with an efficient Fourier transform method for solving the equation. His method has been widely used to model sound propagation in the ocean. Where sound interacts weakly with the bottom, the method is fast and accurate, but in cases where bottom interaction is strong, the method is considerably slower and less accurate. Consequently, new PE methods have been developed that efficiently and accurately account for strong bottom interaction. This paper discusses two important improvements: the first improvement is a more accurate approximation for the phase of bottom-interacting sound, and the second is accurate treatment of boundary conditions in the bottom. PE calculations with and without these improvements have been compared with exact benchmark results for test cases with strong bottom interaction. The improved calculations are in excellent agreement with the exact results whereas the unimproved calculations show only marginal agreement.

## 1. Introduction

A useful approach for calculating underwater sound propagation in a range-dependent environment was introduced by Tappert [1,2,3,4], who used a parabolic equation (PE) method to solve the acoustic wave equation. Tappert's PE approximation transforms the acoustic wave equation, which is an elliptic partial differential equation, into a parabolic partial differential equation. The resulting PE governs the outgoing field and can be solved by the split-step Fourier algorithm developed by Tappert. The split-step algorithm solves the parabolic wave equation by imposing an artificial zero bottom boundary condition and pressure release surface condition; therefore, it solves a pure initial value problem. In cases where the bottom interaction is strong, a more general purpose solution is useful for handling a bottom boundary condition. For this reason, Lee, Botseas, and Papadakis [5,6] developed an Implicit Finite-Difference (IFD) scheme as well as an Ordinary-Differential-Equation (ODE) method to solve Tappert's parabolic wave equation. Their schemes are designed to treat the bottom boundary condition exactly.

The equation introduced by Tappert is approximately limited to propagation angles of less than  $15^\circ$ . For wide angle ( $> 15^\circ$ ) propagation, Tappert's equation can introduce large phase errors into the solution; furthermore, it is with wide angle propagation that strong bottom interaction generally takes place. Consequently, accurate treatment of bottom boundary conditions and wide angle propagation are closely related problems. This paper reports recent improvements in modeling wide angle propagation and discusses improved treatment of boundary conditions at interfaces and at the bottom of the computational grid. Calculations with and without these improvements are compared with exact benchmark results for cases with strong bottom interaction.

## 2. Solution Background

We begin by discussing a numerical solution to a parabolic partial differential equation of the following form:

$$u_r = a(k_0, r, z) u + b(k_0, r, z) u_{zz} \quad (1)$$

with

$$\text{initial conditions } u(0, z) = u_1(z) \quad (2)$$

$$\text{surface boundary condition } u(r, 0) = f_s(r) \quad (3)$$

$$\text{bottom boundary condition } u(r, z_B) = f_B(r) \quad (4)$$

We regard problem (1), associated with conditions (2) through (4), as a well-posed initial boundary value problem in the sense of Hadamard; therefore, we can expect the existence and the uniqueness of the solution.

The parabolic partial differential equation of the form (1) arises in the application of range-dependent underwater acoustic wave propagation problems. The parabolic partial differential equation governing the underwater acoustic wave propagation has the coefficients

$$a(k_0, r, z) = \frac{1}{2} i k_0 [n^2(r, z) - 1] \quad (5)$$

$$b(k_0, r, z) = \frac{i}{2k_0} \quad (6)$$

where  $k$  is a reference wavenumber which equals  $2\pi f/c_0$  and  $c_0$  is a reference sound speed,  $n(r,z) = c_0/c(r,z)$  is the index of refraction, and  $c(r,z)$  is the sound speed profile.

Equation (1) with coefficients as defined by equations (5) and (6) is the conventional parabolic wave equation introduced by Tappert [4]. Tappert introduced a useful technique, called the "artificial bottom," to treat the bottom boundary condition. This technique extends the bottom of the computational grid down deep and adds strong attenuation or truncates the field in the artificial bottom region. For this treatment, the field  $u(r,z)$  goes to zero in the artificial bottom. Thus, for a pressure release surface [ $u(r,0)=0$ ], we see that  $f_s(r)$  of equation (3) and  $f_B(r)$  of equation (4) are both zero; therefore, equation (1) is treated as an initial value problem. The new developments presented in this paper relax the requirement of truncating the field in the bottom by solving an initial boundary value problem for equation (1). Details of the treatment of a homogeneous Neumann boundary condition can be found in reference [7].

Equation (1) is approximately limited to propagation angles of less than about  $15^\circ$ . An improved equation can be derived that accurately treats higher angles and is numerically as simple to solve as equation (1) [8,9]. The wide angle equation can handle propagation angles of up to  $40^\circ$ , depending on the range of propagation.

#### A. Wide Angle Propagation

Consider the two-way (outgoing and incoming) farfield equation for the acoustic field  $u$ :

$$\left\{ \frac{\partial^2}{\partial r^2} + 2ik_0 \frac{\partial}{\partial r} + \left[ k_0^2(n^2 - 1) + \frac{\partial^2}{\partial z^2} \right] \right\} u = 0. \quad (7)$$

The associated one-way outgoing wave equation is obtained by formally solving equation (7) for  $\partial u / \partial r$ , using the quadratic equation formula:

$$\frac{\partial}{\partial r} u = +i \left[ \sqrt{k_0^2 + k_0^2(n^2 - 1) + \frac{\partial^2}{\partial z^2}} - k_0 \right] u. \quad (8)$$

In equation (8) the "+" sign has been chosen so that outgoing waves are represented. For a range-independent medium, equation (8) is exact; that is, a solution of equation (8) is also a solution of equation (7). Now write

$$Q = k_0^2 + k_0^2(n^2 - 1) + \frac{\partial^2}{\partial z^2} \quad (9)$$

and

$$q = \frac{Q}{k_0^2} - 1. \quad (10)$$

Then equation (8) can be written as

$$\frac{\partial}{\partial r} u = i(\sqrt{Q} - k_0) u. \quad (11)$$

Using a rational function approximation for the square root operator

$$\sqrt{Q} = k_0 \left( \frac{A + Bq}{C + Dq} \right), \quad (11a)$$

we find that

$$\frac{\partial}{\partial r} u = ik_0 \left( \frac{A + Bq}{C + Dq} - 1 \right) u. \quad (12)$$

In equations (11a) and (12) the denominator in the rational approximation means  $(C + Dq)^{-1}$ . Hence, an equivalent equation is

$$(C + Dq) \frac{\partial}{\partial r} u = ik_0 [(A - C) + (B - D)q] u. \quad (13)$$

Claerbout's [10,11] one-way wave equation uses  $A = 1$ ,  $B = 3/4$ ,  $C = 1$ , and  $D = 1/4$ . If we select  $A = 1$ ,  $B = 1/2$ ,  $C = 1$ , and  $D = 0$ , we obtain the Tappert parabolic equation. Claerbout's approximation is equivalent to a quadratic expansion of  $\sqrt{Q}$  whereas Tappert's approximation is a linear expansion.

Assuming  $Q$  is a constant over the interval  $r_1$  and  $r_2$  and using the Crank-Nicolson scheme to solve equation (11), we find that

$$u_2 - u_1 = i(\sqrt{Q} - k_0) \left( \frac{u_2 + u_1}{2} \right) \Delta r \quad (14)$$

where  $\Delta r = r_2 - r_1$ . The resulting implicit equation is

$$\left[ 1 - i(\sqrt{Q} - k_0) \frac{\Delta r}{2} \right] u_2 = \left[ 1 + i(\sqrt{Q} - k_0) \frac{\Delta r}{2} \right] u_1. \quad (15)$$

Using the definition for  $Q$  along with the rational approximation for  $Q$ , we obtain

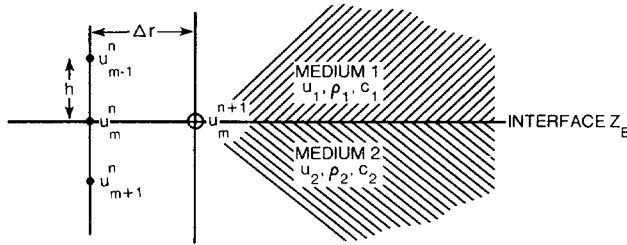
$$\begin{aligned} & \left\{ C + D(n^2 - 1) - \frac{1}{2} \Delta r (ik_0) [(A - C) + (B - D)(n^2 - 1)] \right. \\ & \quad \left. + \left( \frac{D}{k_0^2} - \frac{1}{2} \Delta r \frac{i}{k_0} (B - D) \right) \frac{\partial^2}{\partial z^2} \right\} u_2 \\ & = \left\{ C + D(n^2 - 1) + \frac{1}{2} \Delta r (ik_0) [(A - C) + (B - D)(n^2 - 1)] \right. \\ & \quad \left. + \left( \frac{D}{k_0^2} + \frac{1}{2} \Delta r \frac{i}{k_0} (B - D) \right) \frac{\partial^2}{\partial z^2} \right\} u_1. \quad (15a) \end{aligned}$$

Claerbout's approximation for  $\sqrt{Q}$  is considerably more accurate than Tappert's. Consequently,

equation (15a) with Claerbout's coefficients propagates high-angle waves more accurately than does the conventional parabolic equation. In most problems, the phase errors that are present with the conventional PE are eliminated in Claerbout's equation.

#### B. A Treatment of the Horizontal Interface Condition

The boundary condition at the interface between two media requires the continuity both of the pressure and of the normal component of particle velocity (see figure 1).



The Interface Between Two Media  
Figure 1

These requirements give rise to the following two interface conditions:

(1) Continuity of pressure

$$u_1(r, z_B) = u_2(r, z_B); \quad (16)$$

(2) Continuity of normal component of particle velocity

$$\rho_2 \left. \frac{\partial u_1}{\partial z} \right|_{z=z_B} = \rho_1 \left. \frac{\partial u_2}{\partial z} \right|_{z=z_B} \quad (17)$$

McDaniel and Lee [12] applied an implicit finite-difference technique to derive a parabolic equation to describe the wave field at an interface:

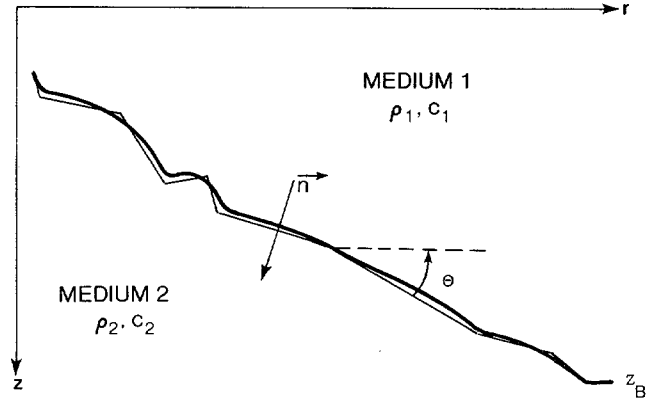
$$u_r = \left( \frac{1}{b_1} + \frac{\rho_1}{\rho_2} \frac{1}{b_2} \right)^{-1} \left\{ \left( \frac{a_1}{b_1} + \frac{\rho_1}{\rho_2} \frac{a_2}{b_2} \right) u + \frac{2}{h^2} \left[ \frac{\rho_1}{\rho_2} (u_{m+1}^n - u) - (u - u_{m-1}^n) \right] \right\} \quad (18)$$

where  $u_1 = u_2 = u$  on the interface.

The densities and grid-point values of  $u$  are defined in figure 1. The functions  $a_1$ ,  $a_2$ ,  $b_1$ , and  $b_2$  are  $a(k_0, r, z)$  and  $b(k_0, r, z)$  at media 1 and 2, respectively.

#### C. A Homogeneous Neumann Boundary Condition

Whenever an irregular bottom boundary profile exists, we use a linear line segmentation to represent the bottom profile. This is shown below in figure 2.



An Irregular Boundary Profile  
Figure 2

The above linearization process, which permits automatic handling of the horizontal boundary, also gives a systematic way to treat a sloping bottom. Suppose the sloping boundary makes an angle  $\theta$  with the horizontal, then, the outward normal derivative operator is expressed by  $\partial/\partial z \cos \theta - \partial/\partial r \sin \theta$ . Let  $p(r, z)$  be the wave field of the reduced wave equation such that  $p(r, z) = H_0^{(1)}(k_0 r) u(r, z)$  where  $H_0^{(1)}(k_0 r)$  stands for the zeroth order Hankel function of the first kind. The homogeneous Neumann bottom boundary condition requires that  $p_N = 0$  on the bottom boundary. Applying the normal derivative operator to the wave field  $p$ , we obtain

$$\frac{\partial p}{\partial z} \cos \theta - \frac{\partial p}{\partial r} \sin \theta = 0 \quad (19)$$

Substituting  $p(r, z) = H_0^{(1)}(k_0 r) u(r, z)$  into (19), we see that the field  $u(r, z)$  not only satisfies (1), but also satisfies the Neumann boundary condition at the bottom. Using equation (1) for  $\partial u/\partial r$  and substituting it into equation (19), we obtain

$$H_0^{(1)}(k_0 r) \frac{\partial u}{\partial z} \cos \theta - \left[ H_0^{(1)}(k_0 r) \right]_r \sin \theta u - H_0^{(1)}(k_0 r) \sin \theta \left( a u + b \frac{\partial^2 u}{\partial z^2} \right) = 0 \quad (20)$$

Upon rearranging the coefficients, we express equation (20) in the form:

$$u_{zz} + p_1 u_z + p_2 u = 0 \quad (21)$$

Equation (21) is a second-order ordinary differential equation, which we treat as an initial value problem with

$$p_1 = -\frac{\cot \theta}{b(k_o, r, z)} \quad (22)$$

$$p_2 = \left[ \frac{\left( H_o^{(1)}(k_o r) \right)_r}{H_o^{(1)}(k_o r)} + a(k_o, r, z) \right] / b(k_o, r, z) \quad (23)$$

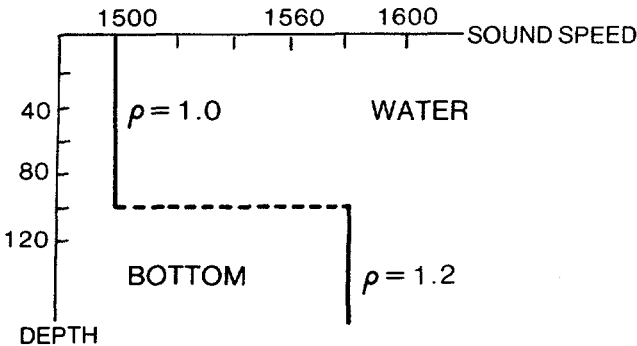
and initial values  $u(r, z_B)$  and  $\frac{\partial u}{\partial z} \Big|_{z_B}$ .

The Neumann bottom boundary condition as well as the wide angle capability and the horizontal interface condition have been incorporated into the IFD model. Examples compared with benchmark solutions are given in the next section. Except as noted, the PE solution deals with the Tappert equation.

### 3. Examples

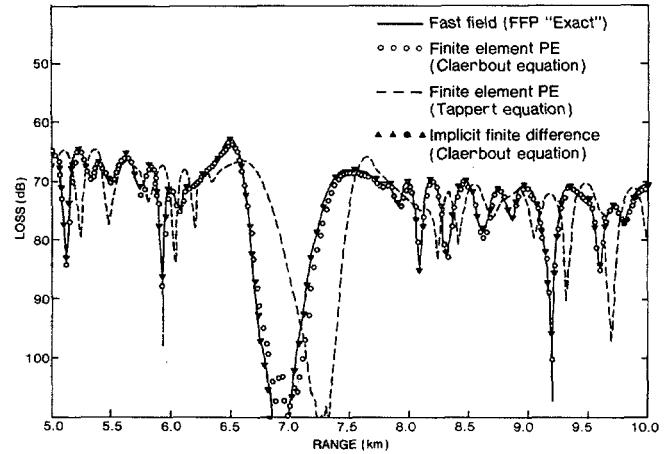
#### A. A Wide Angle Propagation

This problem has a range-independent environment and consists of an isovelocity water column over an isovelocity half-space bottom. Both the source and the receiver are placed at the same depth, 90.5 m below the surface. The source frequency is 250 Hz. The sound speed profile is described by figure 3, where the sound speed is 1500 m/s in the water column and 1590 m/s in the bottom. There is a density change from the water column to the bottom: from 1.0 gm/cm<sup>3</sup> in the water to 1.2 gm/cm<sup>3</sup> in the bottom. The attenuation in the water is zero, and the bottom attenuation is 0.5 dB/λ. The propagation loss was calculated up to a maximum range of 10 km. The maximum propagation angle for this problem is calculated to be approximately 19°; therefore, the wide-angle capability is important.



Sound Speed Profile  
Figure 3

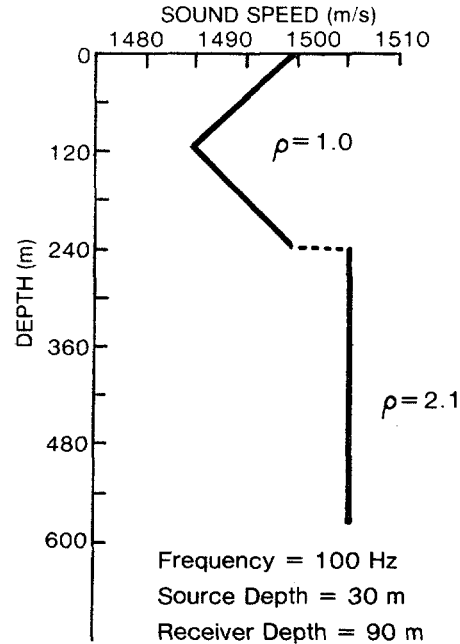
A fast field [13] exact solution is used as a benchmark solution and a finite element [8] solution is used as a reference solution. As shown in figure 4, without the wide angle capability, a phase error is evident; however, with the wide angle capability, the IFD model gives excellent agreement with both the fast field solution and the finite element solution.



Wide Angle Solution Comparison  
Figure 4

#### B. Horizontal Interface

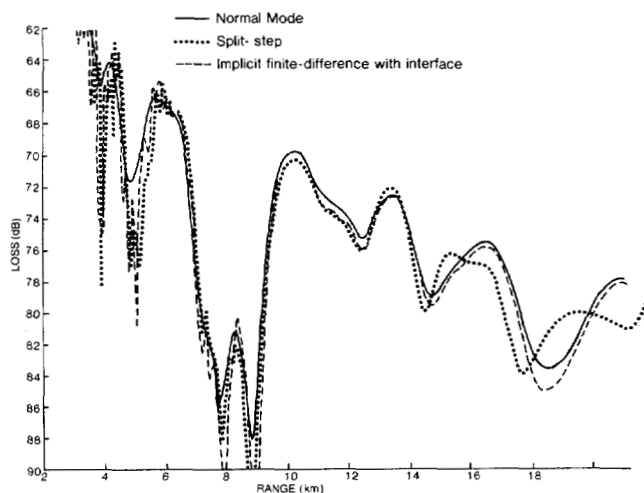
A single interface example is presented. This single interface occurs in a range-independent environment, as shown by figure 5.



Sound Speed Profile  
Figure 5

A 100 Hz source is placed at 30 m below the surface; the receiver is placed at a depth of 90 m. The water-sediment interface occurs at a depth of 240 m. The density in the water column is  $1 \text{ gm/cm}^3$ , and the density in the sediment is  $2.1 \text{ gm/cm}^3$ . The sound speed profile (as shown by figure 5) contains two linear segments in the water column and is a constant of 1505 m/s in the sediment.

Transmission loss is calculated up to a maximum range of 20 km. A normal mode solution [12] is used as a benchmark solution. Numerical results (figure 6) show that the finite-difference method treats the interface more accurately than does the split-step method. The generalization of the treatment to the irregular interface has been worked out by Lee and McDaniel [14]

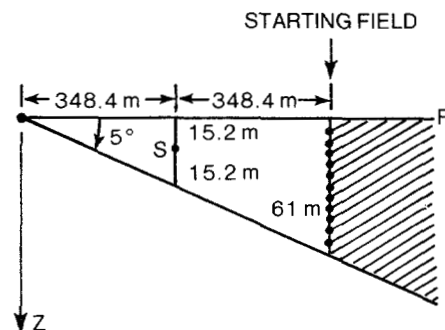


Transmission Loss Numerical Results  
Figure 6

### C. Propagation in a Wedge Region

Figure 7 below describes shallow-to-deep propagation in water bounded by a pressure release surface and a rigid bottom. For a constant sound speed, the exact solution for the acoustic field in a homogeneous medium can be solved by the method of images [15]. We use the exact solution as a benchmark solution.

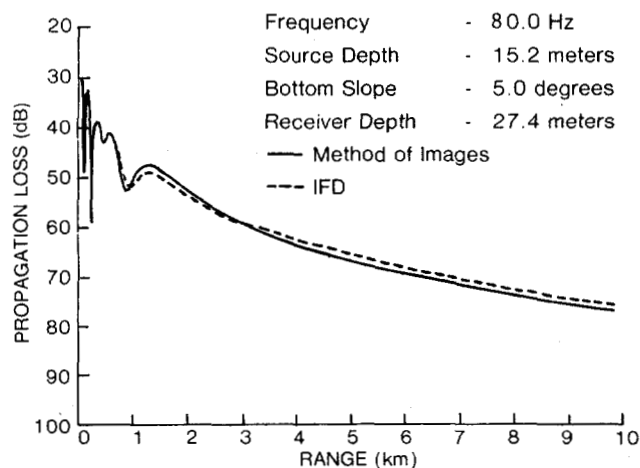
The source is placed at 15.2 m below the surface with a frequency of 80 Hz at the initial depth of 30.4 m. The wedge angle is  $5^\circ$ . The sound speed is a constant 1524 m/s; therefore, the reference sound speed is also 1524 m/s. The sound is propagated to a range of 10 km.



Shallow-to-Deep Water Propagation  
Figure 7

The pressure release surface condition defines the acoustic field to be zero everywhere at the surface. The homogeneous Neumann bottom boundary condition requires that the normal derivative of the wave field  $p(r,z)$  equals zero. The solution field on the bottom boundary is obtained by solving second-order ordinary differential equation (21), which we just developed.

The solution to this problem requires a variable-dimension procedure in order to march out in range because this is a downward sloping bottom. The variable-dimension procedure adjusts the system of equations one dimension higher than the previous dimension after the procedure has advanced one range increment. To ensure simplicity, the range step size  $\Delta r$  is selected arbitrarily as  $\Delta z \cot 5^\circ$ . This selection ensures a uniform depth partition at every range and permits the solution to be produced systematically. The solution comparison is given by figure 8. The IFD solution shows excellent agreement with the exact solution. No comparison is made against the split-step method because existing split-step models cannot treat this problem.



Wedge Solution Comparison  
Figure 8

#### 4. Discussion

The PE approximation is a useful tool for solving the acoustic wave equation in a range-dependent environment. PE models that use the split-step Fourier algorithm have difficulty in handling strong bottom interaction and wide angle propagation. Other models such as the finite-difference scheme [16], the ordinary-differential-equation methods, and the finite-element methods offer more accuracy and more generality. As more capabilities are built into the PE model, a larger class of underwater acoustic wave propagation problems can be solved. Hence, the development of these capabilities should be of great interest to PE users as well as to PE developers.

#### 5. Acknowledgment

This work is jointly supported by NUSC and NORDA.

#### 6. References

1. F. D. Tappert and R. H. Hardin, "Application of the Split-step Fourier method to the numerical solution of nonlinear and variable coefficient wave equations," SIAM rev. 15, p. 423, 1973.
2. F. D. Tappert and R. H. Hardin, in A Synopsis of the AESD Workshop on Acoustic Modeling by Non-Ray Tracing Techniques, C. W. Spofford, AESD TN-73-05, Arlington, Va. 1973.
3. F. D. Tappert and R. H. Hardin, "Computer Simulation of Long-Range Ocean Acoustic Propagation Using the Parabolic Equation Method," Eighth International Congress on Acoustics, p. 452, 1974.
4. F. D. Tappert, "The Parabolic Approximation Method," in Wave Propagation and Underwater Acoustics, edited by J. B. Keller and J. S. Papadakis, Lecture Notes in Physics, Vol. 70, Springer-Verlag, Heidelberg, 1977.
5. D. Lee, G. Botseas, and J. S. Papadakis, "Finite-Difference Solutions to the Parabolic Wave Equation," J. Acoust. Soc. Am., 70(3), pp. 795-800, 1981.
6. D. Lee and J. S. Papadakis, "Numerical Solutions for the Parabolic Wave Equation: An Ordinary-Differential-Equation Approach," J. Acoust. Soc. Am., 68, pp. 1482-1488, 1980.
7. D. Lee and S. Preiser, "Generalized Adams Methods for Solving Underwater Wave Propagation Problems," J. Comp. & Maths with Appls., vol. 7, pp. 195-202, 1981.
8. K. E. Gilbert, "Parabolic Equation Workshop," editor J. A. Davis, Naval Ocean Research and Development Activity, TN-143, (in preparation) 1982.
9. R. Greene, "Parabolic Equation Workshop," editor J. A. Davis, Naval Ocean Research and Development Activity, TN-143 (in preparation) 1982.
10. J. F. Claerbout, Fundamentals of Geophysical Data Processing, McGraw-Hill Co., New York, pp. 206, 207, 1976.
11. A. J. Berkhout, "Wave field extrapolation techniques in seismic migration, a tutorial," Geophysics, vol. 46, no. 12, pp. 1638-1656, 1981.
12. S. T. McDaniel and D. Lee, "A Finite-Difference Treatment of Interface Conditions for the Parabolic Wave Equation: The Horizontal Interface," J. Acoust. Soc. Am., 71(4) pp. 855-859, 1982.
13. J. A. Davis, "Parabolic Equation Workshop," Naval Ocean Research and Development Activity, TN-143, (in preparation) 1982.
14. D. Lee and S. T. McDaniel, "A Finite-Difference Treatment of Interface Conditions for the Irregular Interface," Submitted to J. Acoust. Soc. Am., 1982.
15. R. B. Lauer, R. L. Deavenport, and D. M. Potter, "The Acoustic Field in a Homogeneous Wedge as Given by the Method of Images," Naval Underwater Systems Center, TM No. TA11-88-75, 1975.
16. D. Lee and G. Botseas, IFD: An Implicit Finite Difference Computer Model for Solving the Parabolic Equation, Naval Underwater Systems Center, TR 6659, 1982.